Journal of the Korean Crystal Growth and Crystal Technology
Vol. 22, No. 1 (2012) 29-35
http://dx.doi.org/10.6111/JKCGCT.2012.22.1.029

Importance of convection during physical vapor transport of Hg_2Cl_2 in the presence of Kr under environments of high gravitational accelerations

Geug-Tae Kim†

Department of Nano-Bio Chemical Engineering, Hannam University, Taejon 305-811, Korea

(Received December 8, 2011)
(Revised December 23, 2011)
(Accepted January 6, 2012)

Abstract Special attention in the role of convection in vapor crystal growth has been paid since some single crystals under high gravity acceleration of $10g_0$ appear considerably larger than those under normal gravity acceleration ($1g_0$). With increasing the gravity acceleration from $1g_0$ up to $10g_0$, the total molar flux for $\Delta T = 30$ K increases by a factor of 4, while for $\Delta T = 90$, by a factor of 3. The maximum molar fluxes for three different gravity levels of $1g_0$, $4g_0$ and $10g_0$, appear approximately in the neighborhood of $y = 0.5$ cm, and the molar fluxes show asymmetrical patterns, which indicate the occurrence of either one single or more than one convective cell. As the gravitational level is enhanced form $1g_0$ up to $10g_0$, the intensity of convection is increased significantly through the maximum molar fluxes for $\Delta T = 30$ K and 90 K. At $10g_0$, the maximum total molar flux is nearly invariant for for $\Delta T = 30$ K and 90 K. The total molar flux increases with increasing the gravity acceleration, for $1g_0 \le g_y \le 10g_0$, and decreases with increasing the partial pressure of component B, a noble gas called as Kr (Krypton), P_B. The $|U|_{max}$ is directly proportional to the gravity acceleration for 20 Torr $P_B \le 300$ Torr. As the partial pressure of P_B (Torr) decreases from 300 Torr to 20 Torr, the slopes of the $|U|_{max}$s versus the gravity accelerations increase from 0.29 sec to 0.54 sec, i.e. by a factor of 2. The total molar flux of Hg_2Cl_2 is first order exponentially decayed with increasing the partial pressure of component B, P_B (Torr) from 20 Torr up to 300 Torr.

Key words Mercurous chloride, Convection, Krypton, Gravity, Physical vapor transport

1. Introduction

Physical vapor transport (PVT) has become an important crystal growth process for a variety of acousto-optic materials. Of particular importance is the use of PVT for materials processing experiments in high gravity environments, which would provide a better and thorough understanding of transport phenomena occurring in the vapor phase and crystal growth phenomena. Until now many theoretical studies and quantitative experiments on transport phenomena in PVT have been extensively investigated. Most important theoretical works were achieved by Rosenberger *et al*. [1-6] and, recently extended for transition to chaos flow fields in specialty materials of mercurous chloride in applications of microgravity experiments by Duval [7-12]. They have addressed the underlying phenomena in the PVT processes on the relative importance and influencing parameters of diffusion-advection, thermal and/or solutal convection on mass transport. Our recent studies [13-17] are for PVT processes of specialty materials such as mercurous halides under normal and microgravity environments to investigate the role of convection on the mass transport rate and its transition from diffusion-dominated to circulatory convection-dominated regimes in relation to total pressure, temperatures of source and crystal ends, aspect ratio (transport length-to-width), wall temperature profiles, molecular weights.

It is the purpose of this paper to study the transport phenomena covering the various gravity accelerations in the PVT processes of Hg_2Cl_2 crystal growth system. For this theoretical analysis of the PVT processes, a two-dimensional model is in horizontally oriented, cylindrical, closed ampoules in a two-zone furnace system. The effects of high gravity accelerations on solutally and/or thermally buoyancy-driven convection will be considered at this point, primarily for a mixture of Hg_2Cl_2 vapor and impurity of Krypton (Kr) under high gravity conditions.

2. The Model

Mercurous chloride (Hg_2Cl_2) materials are important for applications in acousto-optic and opto-electronic devices such as Bragg cells, X-ray detectors operating at ambient temperature [11]. The equimolar Hg_2Cl_2 com-

†Corresponding author
Tel: +82-42-629-8837
Fax: +82-42-629-8835
E-mail: gtkim@hnu.kr

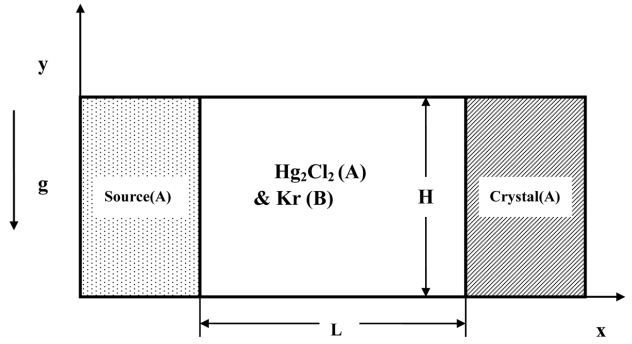

Fig. 1. Schematic and coordinates for a PVT crystal growth reactor of Hg_2Cl_2-Kr in a two-dimensional rectangular system.

pound decomposes to two liquids at a temperature near 525°C where the vapor pressure is above 20 atm [18]. Because of this decomposition and high vapor pressure, Hg_2Cl_2 cannot be solidified as a single crystal directly from the stoichiometric melt. However, very similar to the mercurous bromide, mercurous chloride exhibits sufficiently high vapor pressure at low temperatures so that these crystals are usually grown by the physical vapor transport (PVT) in closed silica glass ampoules.

Consider a rectangular enclosure of height H and transport length L, shown in Fig. 1. The source is maintained at a temperature T_s, while the growing crystal is at a temperature T_c, with $T_s > T_c$. PVT of the transported component A (Hg_2Cl_2) occurs inevitably, due to presence of impurities, with the presence of a component B (Kr). The interfaces are assumed to be flat for simplicity. The finite normal velocities at the interfaces can be expressed by Stefan flow deduced from the one-dimensional diffusion-limited model [19], which would provide the coupling between the fluid dynamics and species calculations. On the other hand, the tangential component of the mass average velocity of the vapor at the interfaces vanishes. Thermodynamic equilibria are assumed at the interfaces so that the mass fractions at the interfaces are kept constant at $\omega_{A,s}$ and $\omega_{A,c}$. On the vertical non-reacting walls appropriate velocity boundary conditions are no-slip, the normal concentration gradients are zero, and wall temperatures are imposed as nonlinear temperature gradients. The density is assumed to be a function of both temperature and concentration. The ideal gas law and Dalton's law of partial pressures are used. Viscous energy dissipation and the Soret-Dufour (thermo-diffusion) effects can be neglected, as their contributions remain relatively insignificant for the conditions encountered in our PVT crystal growth processes. The transport of fluid within a rectangular PVT crystal growth reactor is governed by a system of elliptic, coupled conservation equations for mass (continuity), momentum, energy and species (diffusion) can be represented by the generic equations, Eq. (1) through (4) [20] with their appropriate boundary conditions, Eq. (5) through (7). Let u_x, u_y denote the velocity components along the x- and y-coordinates in the x, y rectangular coordinate, and let T, ω_A, p denote the temperature, mass fraction of species A (Hg_2Cl_2) and pressure, respectively, where the superscript of * denotes the dimensionless [13-17]. The linear temperature profiles at wall boundary conditions only are considered.

$$\nabla^* \bullet \vec{V}^* = 0, \tag{1}$$

$$\vec{V}^* \bullet \nabla^* \vec{V}^* = -\nabla^* P^* + Pr \cdot Ar \nabla^{*2} \vec{V}^* - \frac{Ra \cdot Pr}{Ar} \cdot T^* \cdot e_g, \tag{2}$$

$$\vec{V}^* \bullet \nabla^* T^* = Ar \nabla^{*2} T^* \tag{3}$$

$$\vec{V}^* \bullet \nabla^* \omega_A^* = \frac{Ar}{Le} \nabla^{*2} \omega_A^* \tag{4}$$

On the walls ($0 < x^* < L/H$, $y^* = 0$ and 1):

$$u^*(x^*,0) = u^*(x^*,1) = v^*(x^*,0) = v^*(x^*,1) = 0 \tag{5}$$

$$\frac{\partial \omega_A^*(x^*,0)}{\partial y^*} = \frac{\partial \omega_A^*(x^*,1)}{\partial y^*} = 0,$$

$$T^*(x^*,0) = T^*(x^*,1) = \frac{T - T_c}{T_s - T_c}$$

On the source ($x^* = 0$, $0 < y^* < 1$):

$$u^*(0,y^*) = -\frac{1}{Le} \frac{\Delta\omega}{(1 - \omega_{A,s})} \frac{\partial \omega_A^*(0,y^*)}{\partial x^*}, \tag{6}$$

$$v^*(0,y^*) = 0,$$

$$T^*(0,y^*) = 1,$$

$$\omega_A^*(0,y^*) = 1.$$

Table 1
Typical thermo-physical properties used in this study ($M_A = 472.086$, $M_B = 83.80$)

Transport length, L	10 cm
Aspect ratio (length-to-width, L/H), Ar	5
Source temperature, T_s	350°C
Crystal temperature, T_c	260°C
Prandtl number, Pr	0.80
Lewis number, Le	0.95
Peclet, Pe	4.5
Concentration number, C_v	1.0
Total system pressure, P_T	413.06 Torr
Partial pressure of component B, P_B	20 Torr
Thermal Grashof number, Gr_t	2.99×10^4
Solutal Grashof number, Gr_s	2.66×10^5

On the crystal ($x^* = L/H$, $0 < y^* < 1$):

$$u^*(L/H,y^*) = -\frac{1}{Le(1-\omega_{A,c})}\frac{\Delta\omega}{}\frac{\partial\omega_A^*(L/H,y^*)}{\partial x^*} \quad (7)$$

$$v^*(L/H,y^*) = 0,$$

$$T^*(L/H,y^*) = 0,$$

$$\omega_A^*(L/H,y^*) = 0.$$

3. Results and Discussion

Figure 2 shows the total molar flux of Hg_2Cl_2 in terms of moles $cm^{-2}s^{-1}$ versus gravity acceleration in terms of g_0 (981 cm s^{-2}) for the horizontal orientations for two temperature differences between the source and the crystal regions: ΔT = 30 K (350°C → 320°C, symbol □) and 90 K (350°C → 260°C, symbol ○), based on the parameters of Ar = 5, L = 10 cm, P_B = 20 Torr, with the linear temperatures on the walls. For ΔT = 90 K and $g_y = 1g_0$, the governing dimensionless parameters are as follows: Ar = 5.0, Pr = 0.84, Le = 0.45, $Gr_t = 3.93 \times 10^4$, $Gr_s = 5.47 \times 10^5$, Pe = 3.26, C_v = 1.0. Here, the subscript of 0 denotes the normal gravity acceleration of 981 cm · s^{-2}. With increasing the gravitational acceleration from $1g_0$ up to $10g_0$, the total molar flux for ΔT = 30 K increases by a factor of 4, while for ΔT = 90, by a factor of 3. As depicted in Fig. 2, with increasing from 30 K to 90 K, the corresponding total molar flux is multiplied by a factor of 1.33 for $1g_0 \le g_y \le 10g_0$. It is obvious that the temperature difference between source and crystal is one of the major parameters as well as a driving force for the mass transport during the physical vapor transport. The total molar fluxes versus gravity accelerations vary with a same slope under the condition of same source temperature of 350°C.

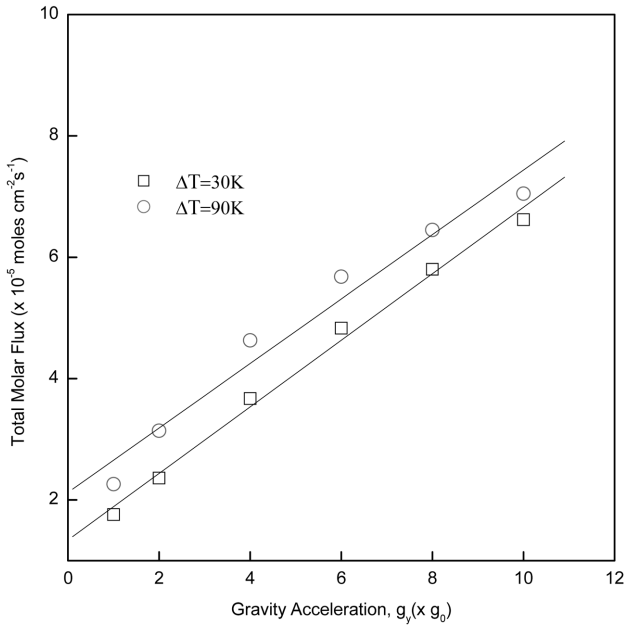

Fig. 2. The total molar flux of Hg_2Cl_2 in terms of moles $cm^{-2}s^{-1}$ versus gravity acceleration in terms of g_0 (981 cm s^{-2}) for the horizontal orientations for two temperature differences between the source and the crystal regions: ΔT = 30 K (350°C → 320°C, symbol □) and 90 K (350°C → 260°C, symbol ○), based on Ar = 5, P_B = 20 Torr, L = 10 cm, with the linear temperature profiles at walls.

This suggests that the effects of thermally buoyancy driven convection is much important even in high gravity environments. The conditions except for the temperature difference remain unchanged and the source temperature of 350°C is fixed so that the effects of thermo-physical properties due to the variations in temperature could be negligible. Note that in actual crystal experiments of Hg_2Cl_2, the typical source and crystal temperature correspond to 320°C and 290°C, respectively.

Figure 3 shows the $|U|_{max}$ as a function of gravity acceleration for two cases of ΔT = 30 K and 90 K, corresponding to Fig. 2. The $|U|_{max}$ is the dimensional maximum magnitude of the velocity vector, which indicates the intensity of convection in the vapor phase. The $|U|_{max}$ has a direct proportional and linear relationship with the gravity acceleration. The two cases of ΔT = 30 K and 90 K have a gradient of 0.22 and 0.33 cm s^{-1} g_0^{-1}, respectively. The $|U|_{max}$ is not increased by a factor of 3 as the temperature difference is increased by a fac-

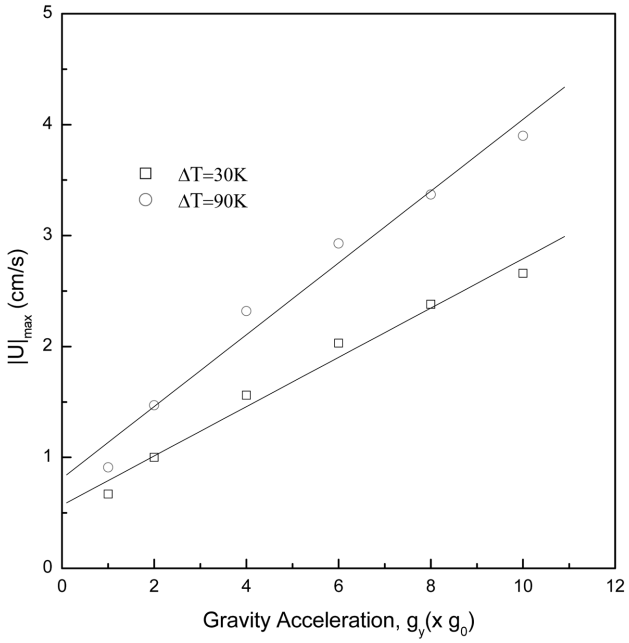

Fig. 3. The $|U|_{max}$ as a function of gravity acceleration for two cases of ΔT = 30 K and 90 K, corresponding to Fig. 2.

tor of 3, but increased by a factor of 1.5 from $\Delta T = 30$ K to 90 K. In addition, the difference between $|U|_{max}$ at $\Delta T = 30$ K and 90 K is significantly enhanced by increasing the level of gravity acceleration for the range from $1g_0$ up to $10g_0$.

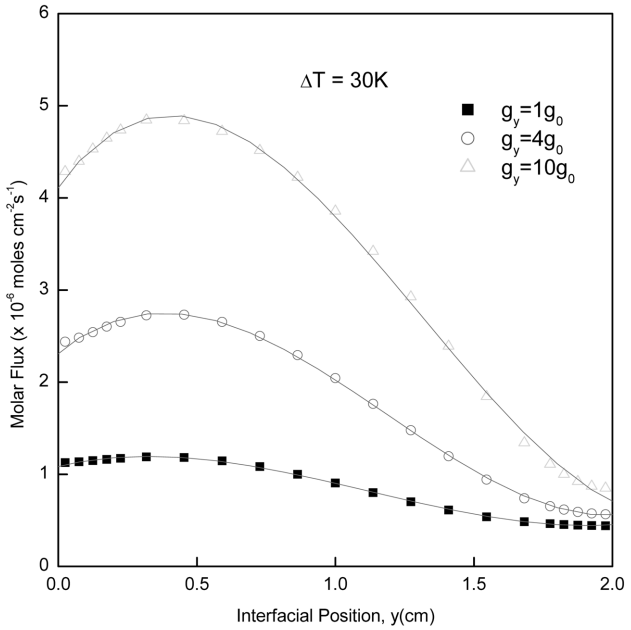

Fig. 4. Interfacial distributions of molar flux of Hg_2Cl_2 for various gravity accelerations, based on $\Delta T = 30$ K, $P_B = 20$ Torr, Ar = 5.0, Pr = 0.84, Le = 0.45, $Gr_t = 3.9 \times 10^4$, $Gr_s = 5.4 \times 10^5$, Pe = 3.26, $C_v = 1$, $g_y = 1g_0$.

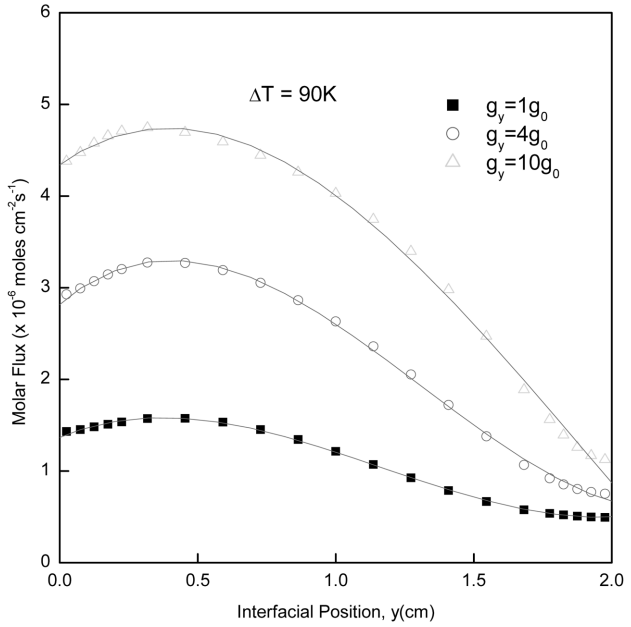

Fig. 5. Interfacial distributions of molar flux of Hg_2Cl_2 for various gravity accelerations, based on $\Delta T = 90$ K and $P_B = 20$ Torr, Ar = 5.0, Pr = 0.80, Le = 0.94, $Gr_t = 2.9 \times 10^4$, $Gr_s = 2.6 \times 10^5$, Pe = 4.5, $C_v = 1.0$, $g_y = 1g_0$.

As depicted in Figs. 4 and 5, the interfacial distributions (molar fluxes versus interfacial positions) for three gravity accelerations of $1g_0$, $4g_0$, and $10g_0$ illustrate that the convection mode is predominant over the diffusion for $0 < y < 1.8$ cm. The maximum molar fluxes for three cases appear approximately in the neighborhood of y = 0.5 cm, and the molar fluxes show asymmetrical patterns against at y = 1.0 cm, which indicate the occurrence of either one single or more than one convective cell. For $\Delta T = 30$ K, the maximum molar flux for $10g_0$ is nearly greater than for $1g_0$ by a factor of 4. The molar flux approaches to a specific value of 0.8×10^{-6} moles cm^2 sec^{-1} due to the effects of walls and diffusion. As depicted in Fig. 5, for $\Delta T = 90$ K and $10g_0$, the maximum molar flux is greater than the minimum by a factor of 4. On the other hand, for $\Delta T = 90$ K and $1g_0$, the maximum molar flux is greater than the minimum molar flux by a factor of 2. Moreover, in comparison of Fig. 4 with 5, the discrepancy between the maximum and the minimum molar flux for $\Delta T = 90$ K and $10g_0$ is greater than for $\Delta T = 30$ K by a factor of 4, which indicate the mass transport is convection-dominated with increasing the temperature difference.

Figure 6 shows the effects of partial pressure of component B, P_B (Torr) on the total molar flux of Hg_2Cl_2 in terms of moles $cm^{-2}s^{-1}$ for various gravity accelerations of $1g_0 \le g_y \le 10g_0$ for the horizontal orientations and the

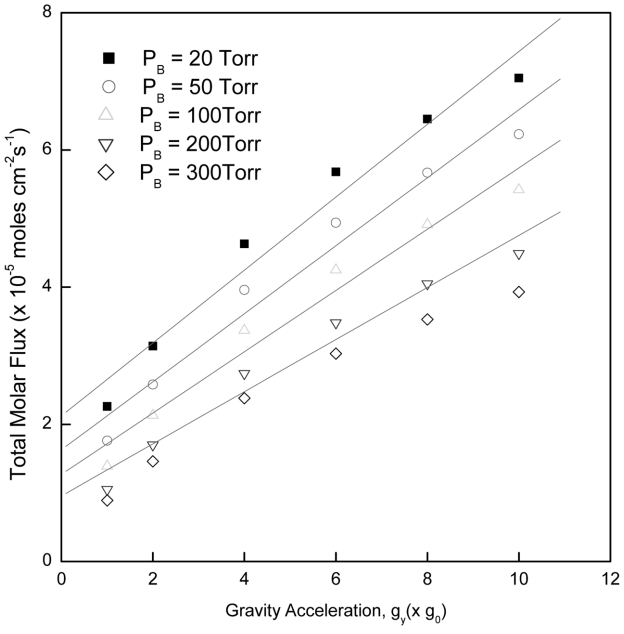

Fig. 6. Effects of partial pressure of component B, P_B (Torr) on the total molar flux of Hg_2Cl_2 in terms of moles $cm^{-2}s^{-1}$ for various gravity accelerations of $1g_0 \le g_y \le 10g_0$ for the horizontal orientations, based on $\Delta T = 90$ K ($350^oC \rightarrow 260^oC$), Ar = 5, L = 10 cm, with the linear temperature profiles at walls.

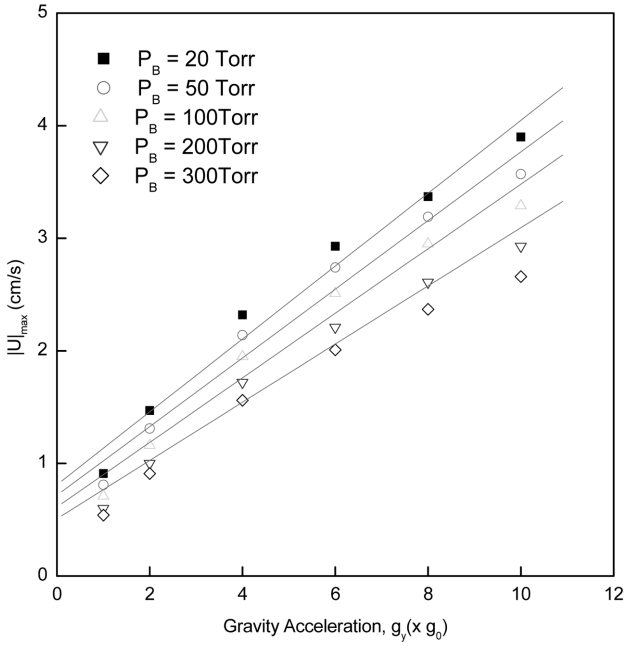

Fig. 7. The $|U|_{max}$ as a function of gravity accelerations for 20 Torr $\leq P_B \leq$ 300 Torr, corresponding to Fig. 6.

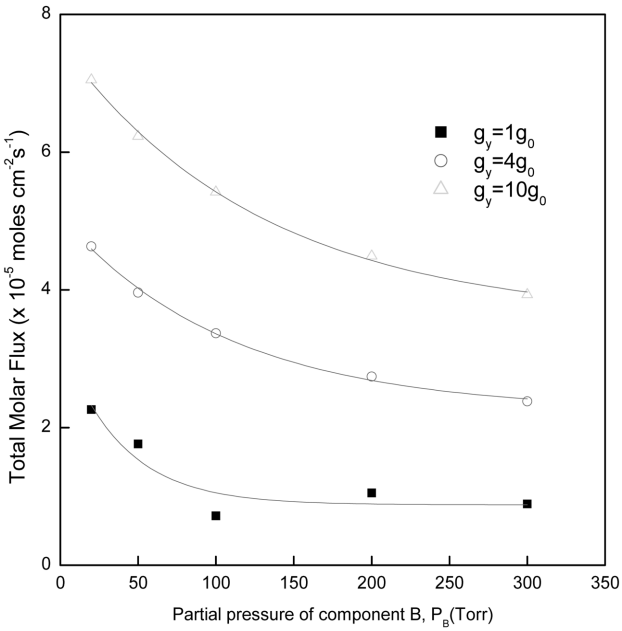

Fig. 8. The total molar flux of Hg_2Cl_2 in terms of moles $cm^{-2}s^{-1}$ as a function of partial pressure of component B, P_B (Torr) for ΔT = 90 K and three gravity accelerations of $g_y = 1g_0$, $4g_0$ and $10g_0$, corresponding to Fig. 6.

temperature differences between the source and the crystal region of 320°C → 290°C, Ar = 5, L = 10 cm, with the linear temperature profiles at walls. As plotted in Fig. 6, the total molar flux increases linearly with increasing the gravitational acceleration, for $1g_0 \leq g_y \leq 10g_0$, and decreases linearly with increasing the partial pressure of component B, Krypton (Kr), P_B. It is clear to see that as the P_B increases from 20 Torr up to 300 Torr for $1g_0 \leq g_y \leq 10g_0$, the gap between the polynomial regression lines is linearly decreased. Figure 7 shows the $|U|_{max}$ as a function of gravitational accelerations for various partial pressures of P_B (Torr), 20 Torr $\leq P_B \leq$ 300 Torr, corresponding to Fig. 6. The $|U|_{max}$ is directly proportional to the gravitational acceleration for 20 Torr $\leq P_B \leq$ 300 Torr. As the partial pressure of P_B (Torr) decreases from 300 Torr to 20 Torr, the slope of the $|U|_{max}$ versus the gravity acceleration increases from 0.23 sec to 0.33 sec. For the gravity accelerations under consideration, the gap between the polynomial regression lines of the $|U|_{max}$ is the smallest at $g_y = 1g_0$, which reflecting the degree of slope for the $|U|_{max}$ versus the gravitational acceleration. In other words, as the P_B (Torr) is increased from 20 Torr to 300 Torr, i.e. by a factor of 15, for $g_y = 10g_0$ and $1g_0$, the $|U|_{max}$ is decreased from 3.9 cm s^{-1} to 2.6 cm s^{-1} by a factor of 0.66, and from 0.91 to 0.54 cm s^{-1} by a factor of 0.59, respectively. Consequently, with increasing the gravitational acceleration from $1g_0$ up to $10g_0$, the ratio of factors for $|U|_{max}$ is increased from 0.59 to 0.66 cm s^{-1}.

Figure 8 shows the total molar flux of Hg_2Cl_2 as a function of gravitational accelerations for various partial pressures of P_B (Torr), 20 Torr $\leq P_B \leq$ 300 Torr, corresponding to Fig. 7. The total molar flux decays first order exponentially with the partial pressure of component B, P_B (Torr) for 20 Torr $\leq P_B \leq$ 300 Torr and three cases of $1g_0$, $4g_0$, $10g_0$. At $g_y = 10g_0$, as the P_B (Torr) is increased from 20 Torr to 300 Torr, i.e. by a factor of 15, the total molar flux is decreased from 0.2×10^{-5} moles $cm^{-2}s^{-1}$ to 0.05×10^{-5} moles $cm^{-2}s^{-1}$ by a factor of 0.57. On the other hand, at $g_y = 1g_0$, an increase in the P_B (Torr) from 20 Torr to 300 Torr, results in a decrease in the total molar flux from 2.26×10^{-5} to 0.89×10^{-5} moles cm^2 sec^{-1}, i.e., by a factor of 0.39. Therefore, as the gravity level is increased from $1g_0$ to $10g_0$, the ratio of factors for the total molar flux is varied from 0.25×10^{-5} through 0.59×10^{-5} moles cm^2 sec^{-1}.

One can see that the effect of thermo-solutal convection first increases and then decreases rapidly and eventually the mode of transport becomes largely diffusion.

Figure 9 shows the interfacial distributions of molar flux of Hg_2Cl_2 for various gravity accelerations, at ΔT = 90 K and P_B = 200 Torr. The total molar fluxes decrease sharply near P_B = 20 Torr, and, then since P_B = 100 Torr, decrease slowly until at P_B = 300 Torr. At $g_y = 1g_0$, the decrease in the total molar flux appears relatively small for 100 Torr $\leq P_B \leq$ 300 Torr, and the corresponding regres-

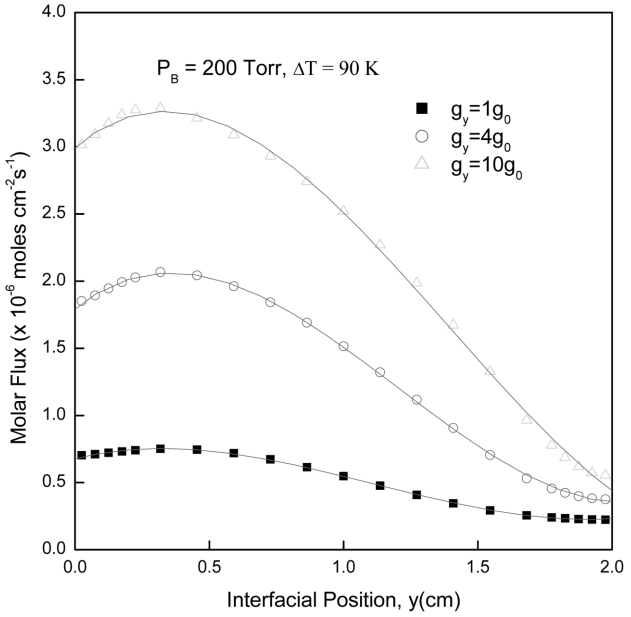

Fig. 9. Interfacial distributions of molar flux of Hg_2Cl_2 for various gravity accelerations, based on $\Delta T = 90$ K and $P_B = 200$ Torr, Ar = 5.0, Pr = 0.74, Le = 0.59, $Gr_t = 1.4\times10^3$, $Gr_s = 1.1 \times 10^5$, Pe = 0.8, $C_v = 1.8$, $g_y = 1g_0$.

sion profile is nearly flat. For the case of $g_y = 1g_0$, P_B = 20 Torr and $\Delta T = 90$ K in Fig. 5, the operation parameters are as follows: Ar = 5.0, Pr = 0.8, Le = 0.94, $Gr_t = 2.9 \times 10^4$, $Gr_s = 2.6 \times 10^5$, Pe = 4.5, $C_v = 1.0$. As shown in Fig. 9, like the cases of $P_B = 20$ Torr, i.e., as shown in Fig. 5, the maximum molar flux for three gravitational accelerations appear at the neighborhood of y = 0.5 cm, and the molar fluxes versus the interfacial positions show asymmetrical against the position of y = 1.0 cm. The molar fluxes for three different gravities of 1, 4, and $10g_0$ converge at the neighborhood of 0.4, while for the cases of $P_B = 20$ Torr, the molar fluxes approach the value of 0.8×10^{-6} moles cm^2 sec^{-1} near y = 2.0 cm. This result indicates that the convection for $P_B = 20$ Torr are likely to be more predominant near y = 2.0 cm than for $P_B = 200$ Torr. In comparison of Figs. 5 and 9, an increase in the partial pressure of component B, P_B from 20 to 200 Torr suppresses the convective effects. The maximum molar flux for $P_B = 20$ Torr and $10g_0$ is greater than for $P_B = 200$ by a factor of 1.39. In addition, for $P_B = 200$ Torr and $10g_0$ in Fig. 9, the maximum molar fluxes is greater than the minimum molar fluxes by a factor of 5.5. The difference between the maximum and the minimum molar flux for $P_B = 20$ Torr and $10g_0$ is greater than for $P_B = 200$ Torr by a factor of 1.4, which implies the mass transport by the diffusion is strong to enough to cause more significant nonuniformities with increasing the partial pressure of component B, P_B.

4. Conclusions

The convection in crystal growth of Hg_2Cl_2-Kr during the physical vapor transport under environments of high gravitational accelerations is strong enough to cause the nonouniformites in front of the crystal region. The levels of gravitational acceleration more than $1g_0$ are appropriate to ensure the mass transport by the means of diffusive-convection. For both $\Delta T = 30$ K and 90 K, the total molar flux increases by a factor of 3.5 with increasing the gravitational acceleration from $1g_0$ up to $10g_0$. The maximum molar fluxes for $1g_0$, $4g_0$ and $10g_0$ appear approximately in the neighborhood of y = 0.5 cm, and the molar flux shows asymmetrical patterns, which indicate the occurrence of either one single or more than one convective cell inside the enclosure. For $P_B = 20$ Tor and $\Delta T = 30$ K, the maximum molar flux for $10g_0$ is nearly greater than that for $1g_0$ by a factor of 4.0. The total molar flux increases with increasing the gravity acceleration, for $1g_0 \le g_y \le 10g_0$, and decreases with increasing the partial pressure of component B, Krypton (Kr), P_B, for 20 Torr $\le P_B \le$ 300 Torr. Also, the $|U|_{max}$ is directly and linearly proportional to the gravity acceleration for 20 Torr $\le P_B \le$ 300 Torr. The total molar flux of Hg_2Cl_2 is first order exponentially decayed with increasing the partial pressure of component B, P_B (Torr) from 20 Torr up to 300 Torr.

Acknowledgments

This work was financially supported by the Hannam University under Grant No. 2011A234 (April 1, 2011 through Feburary 29, 2012).

References

[1] D.W. Greenwell, B.L. Markham and F. Rosenberger, “Numerical modeling of diffusive physical vapor transport in cylindrical ampoules”, J. Crystal Growth 51 (1981) 413.
[2] B.L. Markham, D.W. Greenwell and F. Rosenberger, “Numerical modeling of diffusive-convective physical vapor transport in cylindrical vertical ampoules”, J. Crystal Growth 51 (1981) 426.
[3] B.S. Jhaveri and F. Rosenberger, “Expansive convection in vapor transport across horizontal enclosures”, J. Crystal Growth 57 (1982) 57.
[4] B.L. Markham and F. Rosenberger, “Diffusive-convective vapor transport across horizontal and inclined rectangular enclosures”, J. Crystal Growth 67 (1984) 241.

[5] A. Nadarajah, F. Rosenberger and J. Alexander, "Effects of buoyancy-driven flow and thermal boundary conditions on physical vapor transport", J. Crystal Growth 118 (1992) 49.
[6] F. Rosenberger, J. Ouazzani, I. Viohl and N. Buchan, "Physical vapor transport revised", J. Crystal Growth 171 (1997) 270.
[7] H. Zhou, A. Zebib, S. Trivedi and W.M.B. Duval, "Physical vapor transport of zinc-telluride by dissociative sublimation", J. Crystal Growth 167 (1996) 534.
[8] W.M.B. Duval, "Convection in the physical vapor transport process--I: Thermal convection", J. Chem. Vapor Deposition 2 (1994a) 188.
[9] W.M.B. Duval, "Convection in the physical vapor transport process--II: Thermosolutal convection", J. Chem. Vapor Deposition 2 (1994b) 282.
[10] W.M.B. Duval, "Transition to chaos in the physical vapor transport process--I: fluid mechanics problem phenomena in microgravity", Fluids Eng. Div. ASME 175 (1993) 51.
[11] W.M.B. Duval, N.E. Glicksman and B. Singh, "Physical vapor transport of mercurous chloride crystals; design of a microgravity experiment", J. Crystal Growth 174 (1997) 120.
[12] P.A. Tebbe, S.K. Loyalka and W.M.B. Duval, "Finite element modeling of asymmetric and transient flow fields during physical vapor transport", Finite Elements in Analysis and Design 40 (2004) 1499.
[13] G.T. Kim, W.M.B. Duval, N.B. Singh and M.E. Glicksman "Thermal convective effects on physical vapor transport growth of mercurous chloride crystals (Hg_2C1_2) for axisymmetric 2-D cylindrical enclosure", Modelling. Simul. Mater. Sci. Eng. 3 (1995) 331.
[14] G.T. Kim, W.M.B. Duval and M.E. Glicksman "Thermal convection in physical vapour transport of mercurous chloride (Hg_2Cl_2) for rectangular enclosures", Modelling. Simul. Mater. Sci. Eng. 5 (1997) 289.
[15] G.T. Kim, W.M.B. Duval and M.E. Glicksman "Effects of asymmetric temperature profiles on thermal convection during physical vapor transport of Hg_2Cl_2", Chem. Eng. Comm. 162 (1997) 45.
[16] G.-T. Kim and K.-H. Lee, "Parametric studies on convection during the physical vapor transport of mercurous chloride (Hg_2Cl_2)", J. Korean Crystal Growth and Crystal Technology 14 (2004) 281.
[17] G.T. Kim, "Convective-diffusive transport in mercurous chloride (Hg_2Cl_2) crystal growth", J. Ceramic Processing Research 6 (2005) 110.
[18] S.J. Yosim and S.W. Mayer, "The mercury-mercuric chloride system", J. Phys. Chem. 60 (1960) 909.
[19] F. Rosenberger and G. Müller, "Interfacial transport in crystal growth, a parameter comparison of convective effects", J. Crystal Growth 65 (1983) 91.
[20] S.V. Patankar, "Numerical heat transfer and fluid flow", (Hemisphere Publishing Corp., Washington D.C., 1980).